Available online at www.sciencedirect.com

ScienceDirect

Geochimica et Cosmochimica Acta 275 (2020) 123–139

Geochimica et Cosmochimica Acta

www.elsevier.com/locate/gca

An important biogeochemical link between organic and inorganic carbon cycling: Effects of organic alkalinity on carbonate chemistry in coastal waters influenced by intertidal salt marshes

Shuzhen Song [a,b], Zhaohui Aleck Wang [b,*], Meagan Eagle Gonneea [c], Kevin D. Kroeger [c], Sophie N. Chu [d], Daoji Li [a,*], Haorui Liang [b,e]

[a] State Key Laboratory of Estuarine and Coastal Research, East China Normal University, Shanghai 200241, China
[b] Department of Marine Chemistry and Geochemistry, Woods Hole Oceanographic Institution, Woods Hole, MA 02543, USA
[c] Woods Hole Coastal and Marine Science Center, U. S. Geological Survey, Woods Hole, MA 02543, USA
[d] Joint Institute for the Study of the Atmosphere and Ocean, University of Washington, Seattle, WA 98105, USA
[e] College of Chemistry and Chemical Engineering, Ocean University of China, Qingdao, Shandong 266100, China

Received 14 January 2019; accepted in revised form 13 February 2020; available online 19 February 2020

Abstract

Dissolved organic carbon (DOC) contains organic acid charge groups that contribute organic alkalinity (OrgAlk) to total alkalinity (TA). These effects are often ignored or treated as a calculation uncertainty in many aquatic CO_2 studies. This study evaluated OrgAlk variability, sources, and characteristics in estuarine waters exchanged tidally with a groundwater-influenced salt marsh in the northeast USA. OrgAlk provided a biogeochemical link between organic and inorganic carbon cycling through its direct effects on pH, and thus CO_2 system speciation and buffer capacity. Two main charge groups were identified including carboxylic and phenolic or amine groups. Terrestrial groundwater and in-situ production within salt marsh peat contributed OrgAlk to the tidal creek, with the former being a more significant source. Groundwater entering the marsh complex contained exceptionally high OrgAlk (> 150 μmol kg^{-1}), and these compounds were preferentially preserved within the DOC pool during groundwater transport and mixing with coastal water. OrgAlk:DOC ratios in groundwater and marsh-influenced water varied across space and time. This highlights the insufficiency of using a fixed proportion of DOC to account for organic acid charge groups. Accounting for OrgAlk altered H^+ concentrations by ~1–41 nmol kg^{-1} (equivalent to a pH change of ~0.03–0.26), pCO_2 by ~30–1600 μatm and buffer capacity by ~0.00–0.14 mmol kg^{-1} at the relative OrgAlk contributions of 0.9–4.3% of TA observed in the marsh-influenced tidal water. Thus, OrgAlk may have a significant influence on coastal inorganic carbon cycling. Further theoretical calculations confirm that these concentrations of OrgAlk would have sizable impacts on both carbonate speciation and, ultimately, air-sea CO_2 fluxes in different coastal environments, ranging from estuarine to shelf waters. A new conceptual model linking organic and inorganic carbon cycling for coastal waters is proposed to highlight the sources and sinks of organic acid charge groups, as well as their biogeochemical behaviors and mechanistic control on the CO_2 system.

Keywords: Organic alkalinity; Carbon dioxide; Carbon cycle; Salt marsh; Groundwater; Coastal ocean

* Corresponding authors.
E-mail addresses: zawang@whoi.edu (Z.A. Wang), daojili@sklec.ecnu.edu.cn (D. Li).

https://doi.org/10.1016/j.gca.2020.02.013
0016-7037/

1. INTRODUCTION

Highly productive coastal salt marshes contain large carbon stocks with high rates of storage (18–1713 g C m^{-2} yr^{-1}), and thus play an important role in the coastal carbon cycle (Bauer et al., 2013; Ouyang and Lee, 2014; Holmquist et al., 2018; Najjar et al., 2018). These ecosystems export large quantities of dissolved inorganic carbon (DIC), total alkalinity (TA), and dissolved organic carbon (DOC) to nearby marine systems via tidal exchange (Downing et al., 2009; Wang et al., 2016; Chu et al., 2018), although current estimates of these lateral fluxes still bear large uncertainties (Cai, 2011; Bauer et al., 2013; Najjar et al., 2018). Export of DIC and TA from these coastal vegetated ecosystems significantly affects the carbonate system in adjacent coastal waters (Raymond et al., 2000; Wang and Cai, 2004; Wang et al., 2016).

In both freshwater and seawater, DOC contributions to TA, i.e. organic alkalinity (OrgAlk), affect water pH, carbonate speciation, and buffer capacity (e.g., Cai et al., 1998; Muller and Bleie, 2008; Wang et al., 2013; Wang et al., 2016). Since salt marshes export DOC produced during marsh metabolic processes, elevating DOC in marsh-influenced coastal waters, OrgAlk could be a significant component of TA at these sites. Nevertheless, assessment of OrgAlk content and potential effects in estuarine waters adjacent to salt marshes is lacking.

In natural water, TA is defined as the excess of proton acceptors (bases formed from weak acids with a dissociation constant $K \leq 10^{-4.5}$, corresponding to that of carbonic acid) over proton donors (acids with $K > 10^{-4.5}$) (modified from Dickson, 1981):

$$\begin{aligned} TA = {} & [HCO_3^-] + 2[CO_3^{2-}] + [B(OH)_4^-] + [HPO_4^{2-}] \\ & + 2[PO_4^{3-}] + [SiO(OH)_3^-] + [HS^-] + [NH_3] \\ & + [OrgAlk] + [OH^-] - [H^+]_F - [HF] - [HSO_4^-] \\ & - [H_3PO_4] - [OrgA] \cdots, \end{aligned} \quad (1)$$

where contributions of carbonate (HCO_3^- and CO_3^{2-}) and borate ($B(OH)_4^-$) species usually dominate. Organic acid charge groups (negatively charged species) can contribute to TA as a base (OrgAlk) and/or an acid (OrgA) depending on their equilibrium constants (Muller and Bleie, 2008; Ulfsbo et al., 2015). Since TA is commonly used as one input parameter in thermodynamic CO_2 system calculations, any uncertainty in the definition of TA will lead to uncertainty in determining carbonate speciation.

Organic acid charge groups are often perceived as minor species in natural waters and are commonly omitted during CO_2 system speciation calculations (e.g., Kaltin and Anderson, 2005; Paquay et al., 2007; Butman and Raymond, 2011). Nevertheless, previous studies have shown that OrgAlk can be a significant portion of TA in organic carbon-rich waters such as humic-rich rivers and coastal waters, with concentrations varying from negligible to over 100 μmol kg^{-1} (Cai et al., 1998; Hernández-Ayon et al., 2007; Muller and Bleie, 2008; Kim and Lee, 2009; Wang et al., 2013; Kuliński et al., 2014; Yang et al., 2015; Ko et al., 2016; Hammer et al., 2017). The reported effect of ignoring OrgAlk in CO_2 calculations can range from 10 to 60% underestimation to > 160% overestimation of pCO_2 depending on whether the TA-DIC or TA-pH pair is used (Tishchenko et al., 2006; Hunt et al., 2011; Koeve and Oschlies, 2012; Wang et al., 2013; Kuliński et al., 2014; Abril et al., 2015; Yang et al., 2015). Moreover, the impact of OrgAlk extends beyond a source of calculation uncertainty in the CO_2 system. The biogeochemical cycling of organic acid charge groups directly impacts water pH, and thus carbonate speciation, which may ultimately influence air-water CO_2 exchange and inorganic carbon fluxes (e.g., lateral transport and upwelling). Therefore, we propose that the effects of OrgAlk on the CO_2 system may represent an important biogeochemical linkage between organic and inorganic carbon cycling, especially in organic carbon-rich waters.

Herein, we present the first study of OrgAlk in tidal water exchanged between an estuary and a salt marsh system. The goal was to investigate OrgAlk as a biogeochemical linkage between organic and inorganic carbon cycling by studying the sources and composition of OrgAlk, and quantitatively assessing its impacts on the CO_2 system in marsh-influenced coastal water. A simple titration model was used to identify the charge groups of organic acids. The effect of OrgAlk on the CO_2 system speciation and coastal ocean buffer capacity was assessed by including OrgAlk within the traditional seawater CO_2 system calculations. Finally, a conceptual model, depicting the generation and removal of organic acid charge groups within the DOC pool, provides insights into the biogeochemical regulation of the aquatic CO_2 system through OrgAlk contributions.

2. METHOD

2.1. Study site

Sage Lot Pond (SLP) is an intertidal salt marsh, with minimal human impact and nitrogen loading, located on the eastern side of Waquoit Bay (Fig. 1a and b), a shallow estuary on the south coast of Cape Cod, Massachusetts, U.S.A. Groundwater (GW) discharge is the main form of freshwater input to the coast due to highly permeable glacial sand deposits in the region (Cambareri and Eichner, 1998). The annual flux of GW to the SLP tidal creek, where this study was conducted, is about 6310 m^3 or 0.3% of the mean annual tidal exchange (Wang et al., 2016). The plant community in the SLP marsh is dominated by *Spartina patens, Distichlis spicata,* and *Juncus gerardii* in the high marsh and *Spartina alterniflora* in the low marsh (Moseman-Valtierra et al., 2016) (Fig. 1c). The SLP watershed is forested with a mixture of pitch pine and scrub oak (Fig. 1d).

2.2. Sampling and measurements

The entrance to the SLP tidal creek was instrumented with a YSI EXO2 Sonde (YSI Inc., Ohio, USA) to collect in-situ physical parameters including temperature and water depth (Fig. 1d) (Mann et al., 2019). Time-series bottle samples for TA, DIC, OrgAlk, pH, and DOC were collected hourly at ~0.2 m below the surface at the creek

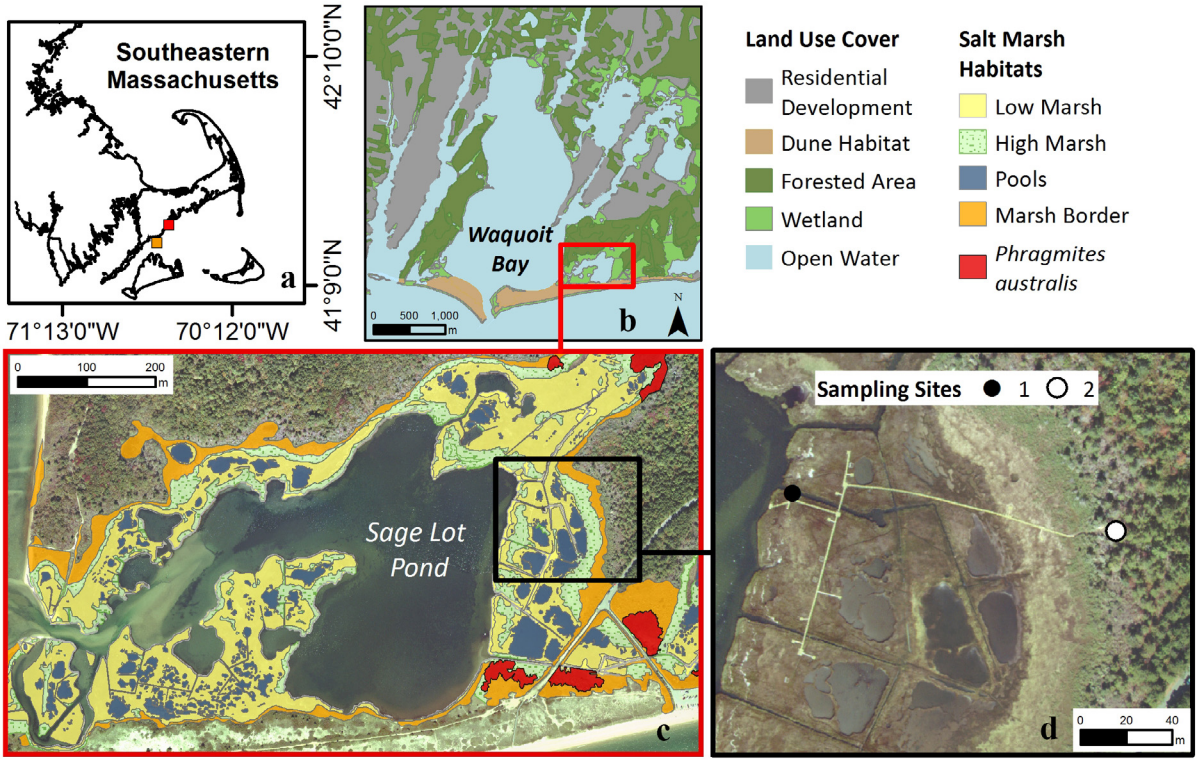

Fig. 1. Study sites. (a) The location of the study area in Massachusetts, USA. Water samples were collected in Waquoit Bay (red square) and Vineyard Sound (orange square); (b) Land use cover map of the Waquoit Bay watershed; (c) Salt marsh habitat map of Sage Lot Pond; (d) The location of sampling sites. Tidal creek water samples were collected at sampling site 1. Ground water (GW) samples were collected at sampling site 2. Maps (b) and (c) are courtesy of Jordan Mora, Waquoit Bay National Estuarine Research Reserve. (For interpretation of the references to color in this figure legend, the reader is referred to the web version of this article.)

mouth over several tidal cycles in May, July, October, and November 2016. The water elevation at the sampling site varied between −0.25 m and 0.64 m (North American Vertical Datum of 1988 or NAVD88), and the water column was well-mixed. Samples for practical salinity (Sp) were collected and analyzed with a Guideline AutoSal instrument at Woods Hole Oceanographic Institution (WHOI). GW was sampled on September 16th, 2016 from a push point sampler installed within the forest adjacent to the marsh at 0.56 m, 0.89 m, and 1.8 m below the land surface to collect OrgAlk, TA, pH, and DOC samples. GW salinity and temperature were measured with a YSI Pro30 (YSI Inc., Ohio, USA) during collection. To constrain the coastal water OrgAlk endmember, two OrgAlk, TA, and pH samples were collected from the WHOI Environmental Systems Laboratory intake, located about 1.6 km offshore in Vineyard Sound (orange square in Fig. 1a), on March 8th and July 9th, 2018, and one DOC sample was collected on March 8th, 2018.

The TA, DIC, and pH sample collection protocol was based on the best practices of seawater CO_2 measurements outlined in Dickson et al. (2007). OrgAlk sample collection followed the TA sampling protocol. In brief, water samples were pumped through 0.45 μm air-tight capsule filters (Farr West Environmental Supply, Texas, USA) and collected into 250 mL borosilicate glass bottles for TA, DIC, pH, and OrgAlk measurements. All samples were filtered to remove particles from the turbid coastal water. These particles interfere with TA, DIC, and pH measurements in several ways, including clogging analytical instruments, interfering with spectrophotometric analyses, and potential inclusion of solid carbonate minerals within the samples. Previous experience indicates that the pressure change that occurs due to our filtering procedure is not likely to change the TA, DIC, and pH values of a sample. Each sample was preserved with 100 μL of a saturated mercuric chloride solution. Samples for DOC analysis were filtered through 0.45 μm pore size polyethersulfone cartridge filters into combusted borosilicate glass vials with Teflon-lined silicone septa caps, acidified to pH < 2 with hydrochloric acid and refrigerated until analysis.

DIC samples were measured with a DIC auto-analyzer (AS-C3, Apollo SciTech Inc., Delaware, USA). Each sample was acidified with 10% phosphoric acid and purged with high purity N_2 gas, and the evolved CO_2 gas was detected and quantified by a LiCOR7000 infrared CO_2 analyzer (LI-COR Environmental, Nebraska, USA). A certified reference material (CRM) from Dr. A. G. Dickson at the Scripps Institution of Oceanography was used for calibration. The precision and accuracy of DIC measurements were both ± 2.0 μmol kg^{-1}.

The pH samples were measured with a UV–visible spectrophotometer (Agilent 8454, Agilent Technologies, USA) at 25 ± 0.1 °C using purified meta-cresol purple (mcp) as

an indicator. The mcp model reported in Douglas and Byrne (2017) was applied to calculate pH across the salinity and temperature ranges in this study. The pH values are reported on the total proton concentration scale and converted from 25 ± 0.1 °C to in-situ temperature using measured DIC and the CO2SYS program (van Heuven et al., 2011). The mean uncertainty of the pH measurement was ±0.006 (range 0.0003–0.017), calculated as the mean difference between duplicate samples ($n = 40$). The difference between pH values of duplicate samples were much higher in samples collected in May and July (mean: 0.007, range: 0.0003–0.017) than those collected in October and November (mean: 0.001, range: 0.0007–0.003). This is likely due to the presence of more colored material, potentially chromophoric dissolved organic matter, and particles smaller than 0.45 μm in May and July samples than the October and November samples that were much clearer. Fine particles and colored material may significantly reduce the accuracy of spectrophotometric pH measurements, and thus affect CO_2 calculation accuracy when pH is used as an input parameter. Alternatively, for future studies in turbid waters (where Sp > 5), sample pH can be measured potentiometrically on the NIST/NBS scale and converted to the total proton concentration scale based on the response of the electrode to TRIS buffer solutions prepared in artificial seawater with similar ionic strengths as the samples (Dinauer and Mucci, 2017).

All TA titrations were conducted at 22.4 ± 0.1 °C using a ROSS^{TM} combination pH electrode. The electrode was calibrated using three buffer solutions on the National Bureau of Standard (NBS) scale (pH = 4.01, 7.00, and 10.01). TA was titrated with a dilute hydrochloric acid (HCl) solution (~0.1 M in 0.7 M NaCl solution) according to a modified Gran titration procedure (Wang and Cai, 2004) using two digital syringe pumps (Kloehn Inc., Las Vegas, USA). HCl concentration was calibrated with the CRM. The mean difference between duplicate samples ($n = 30$) was 2.5 ± 1.9 (one standard deviation) μmol kg^{-1}.

OrgAlk concentration was determined with the same electrode and digital syringe pumps as the TA measurements, based on the procedure reported in Cai et al. (1998) (Fig. 2). Briefly, a 35 g water sample was titrated with a calibrated HCl solution (~0.1 M) until the sample pH was below 3.0 (first titration). CO_2 in the sample was then removed by bubbling with high purity N_2 gas (99.999%) for ~10 min. The acidified sample was then titrated with 0.1 M NaOH solution back to its initial pH (back titration). The NaOH solution was prepared in DI water bubbled with high purity N_2 gas to prevent CO_2 dissolution into the solution. Finally, the sample was titrated with HCl again until its pH was below 3.0 (second titration). During the back titration and second titration, the titration vessel was covered by a plastic bag and continuously flushed with N_2 to maintain a CO_2-free environment. In total, 8–12 points were acquired for the modified Gran titration between 3.0–3.8 pH during the second titration. OrgAlk was calculated as the TA from the second titration minus the borate alkalinity. Borate alkalinity was calculated from salinity, temperature, and sample pH on the NBS scale (Dickson, 1990a; Lee et al., 2010). The mean difference of OrgAlk concentrations between duplicate samples was 2.8 ± 2.1 μmol kg^{-1} ($n = 17$). The total concentrations of sulfide in two low tide water samples in April 2019 were 0–2 μmol kg^{-1}, accounting for 0–1 μmol kg^{-1} sulfide alkalinity. Moreover, sulfide alkalinity could be removed in the form of H_2S along with CO_2 by N_2 bubbling after the first titration. Sulfide alkalinity was thus assumed to be negligible in OrgAlk calculations. Based on nutrient concentration measurements, the contributions of phosphate, ammonium, and silicate to TA were < 1.0 μmol kg^{-1} (Supplementary Data A1) and therefore not considered in OrgAlk calculations.

Even though the NaOH solution was prepared under a N_2-flushed environment, CO_2 may have dissolved into the solution. To determine the residual CO_2 (in the form of CO_3^{2-}), artificial seawater was prepared according to the

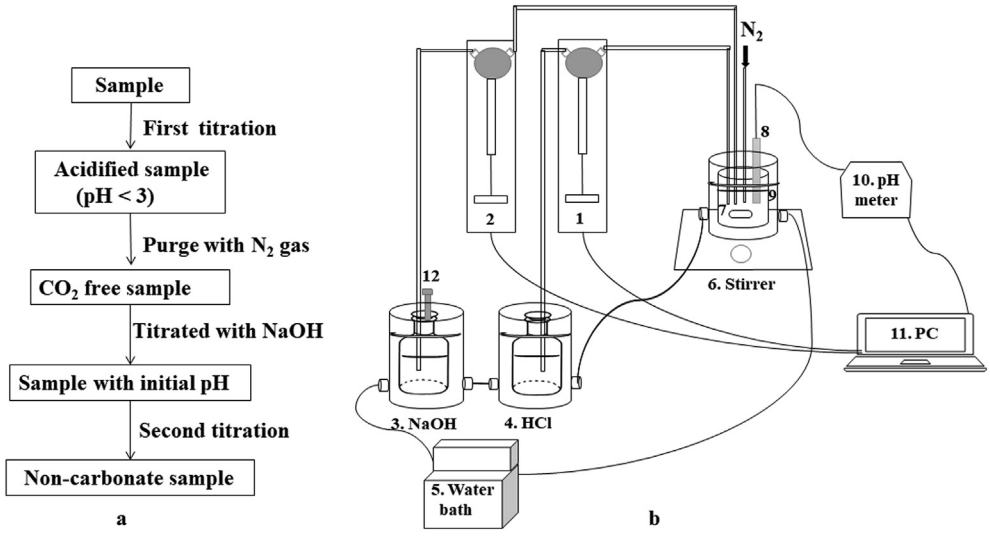

Fig. 2. (a) Flow chart of OrgAlk titration; (b) Schematic of the OrgAlk titration equipment: (1) and (2) Kloehn digital syringe pumps; (3) NaOH solution; (4) HCl solution; (5) Water bath; (6) Magnetic stir; (7) Stir bar; (8) pH electrode; (9) Titration vessel with sample; (10) pH meter; (11) Computer; (12) Soda lime plug.

recipe of Dickson et al. (2007) while excluding bicarbonate/carbonate salts, followed by bubbling with high purity N_2 gas for 4 hours. The carbonate-free artificial seawater was titrated in a similar procedure as OrgAlk. The carbonate ion concentration was calculated as the difference in TA between the first and second titration. The results show that there was $\sim 1.5 \pm 0.2$ mmol L^{-1} CO_3^{2-} ($n = 11$) in the NaOH solution (~0.1 M). The OrgAlk results were corrected by subtracting introduced carbonate alkalinity based on the volume of NaOH solution added during the back titration. For marsh tidal water and Vineyard Sound coastal water samples, there was 12–17 μmol kg^{-1} carbonate alkalinity introduced by the NaOH solution, compared to 21–31 μmol kg^{-1} in GW. The CO_3^{2-} concentration in the NaOH solution measured in this study was similar to that reported by Yang et al. (2015). Although the low ionic strength of the NaOH solution could lead to uncertainties in the determination of OrgAlk in tidal water samples (Sp = 22.8–32.2), we expect this effect to be rather small, as the addition of NaOH solution (214–253 μL) only changed the sample's ionic strength by 0.6–0.7%.

To determine OrgAlk composition in different seasons and end-members, full titrations were also conducted on one or more tidal water samples from each time-series event (excluding October 18th), a GW sample (depth = 0.89 m) and a Vineyard Sound coastal water sample taken ~1 m above the bottom. During a full titration, each sample was first titrated to pH < 3.0, then bubbled with N_2 gas to remove CO_2. Thereafter, the sample was back titrated to pH > 10.0 with ~200 incremental additions of NaOH (0.1 M) at ~1 min intervals over 3 hours.

DOC samples were analyzed on an O. I. Analytical Aurora 1030C Autoanalyzer by high-temperature catalytic oxidation followed by nondispersive infrared detection (HTCO-NDIR). Concentrations are reported relative to a potassium hydrogen phthalate (KHP) standard. Hansell deep seawater (University of Miami Hansell Laboratory, Lot# 01–14), and Suwannee River NOM (IHSS, Lot# 2R101N) reference materials were analyzed daily as additional checks on precision and accuracy of the analyses. Standards and reference materials typically vary by < 5% (precision), with a sample detection limit of 30 μmol kg^{-1}.

2.3. OrgAlk model

A simple model derived from charge balance (Eq. (2)) was established to determine apparent pK values of charge groups during a full titration, with the assumption that all weak organic acids can be characterized by one to three monoprotic weak organic acids (Cai et al., 1998). The carbonate alkalinity of the NaOH solution was also included in the charge balance equation:

$$V_0 \sum_i \frac{X_{iT}}{1+\frac{[H^+]}{K_i}} + \frac{V_0 B_T}{1+\frac{[H^+]}{K_B}} + \frac{VC_{TNa}}{1+\frac{[H^+]}{K_{C1}}+\frac{K_{C2}}{[H^+]}} + \frac{2VC_{TNa}}{1+\frac{[H^+]^2}{K_{C1}K_{C2}}+\frac{[H^+]}{K_{C2}}} -$$

$$(V+V_a)([H^+]-[OH^-]) + V_a C_H^0 - VC_B = 0 \quad (2)$$

where V_0 is the volume of the sample; V_a is the volume of acidified sample after the first titration; V is the total volume of base (NaOH) added during a back titration; K_i, K_B, K_{C1}, and K_{C2} are the dissociation constants of charge group i of organic acids, boric acid, and carbonic acid, respectively. X_{iT} is the total concentration of charge group i of organic acids ($X_{iT} = [HX_i] + [X_i^-]$), B_T is the total concentration of borate, and C_{TNa} is the total concentration of carbonate in the NaOH solution. C_B is the concentration of NaOH, determined through titration with CRM calibrated HCl. C_H^0 is the hydrogen ion concentration after the first titration. K_{C1}, K_{C2}, and K_B were calculated using temperature and salinity using the parameterizations of Cai and Wang (1998) and Dickson (1990a). During the ~3 h back titration step of a full titration, some CO_2 introduced by the NaOH solution might be lost from the sample to the atmosphere, especially when pH was < ~ 6 (i.e., below the pK value of the first dissociation constant of carbonic acid). This could decrease the DIC concentration in the full titration sample. As a result, using the measured carbonate concentration in the NaOH solution (~1.5 mmol L^{-1}, see Section 2.2) to estimate introduced DIC in the full titration samples might result in an over-correction. Instead, we used Eq. (2) to simulate the concentration of CO_3^{2-} in the NaOH solution (C_{TNa}) and the corresponding introduced DIC (VC_{TNa} in Eq. (2)) and carbonate alkalinity (terms 3 and 4 in Eq. (2)) that best fit the titration curve. The parameters X_{iT}, K_i, C_H^0, and C_{TNa} were determined by fitting the nonlinear Eq. (2) using the Matlab™ function 'leastsq' (MathWorks, Inc., USA). First, initial values of K_1, X_{1T}, C_{TNa}, and C_H^0 were determined from data below pH 5.0; then C_H^0 was fixed and a nonlinear fit was performed iteratively for data below pH < ~7.5 to redetermine X_{1T} and K_1. Finally, C_H^0, X_{1T}, and K_1 were fixed, and the values of C_{TNa}, X_{2T}, and K_2 were constrained using all data. A third organic acid charge group was identified, if adding X_{3T} and K_3 improved the fit. The fitting process was considered to be complete when the residual of the fit was less than 0.001 and additional charge groups did not improve the fit.

Assuming zero ionic strength in the samples might introduce uncertainty to pK values of identified organic acid charge groups. Masini et al. (1998) evaluated the magnitude of variation in pK values of twelve types of humic acids (pK values 3–10) at three ionic strengths (I = 0.01, 0.1, 1.0 M). They reported a maximum pK variation of 0.75 over a range of ionic strengths from 0.01 to 1.0 M. The maximum salinity of our full titration sample was 31.5 (I = 0.65 M). If we adopt the estimate by Masini et al. (1998), ignoring ionic strength would result in a maximum error in pK values of 0.49 (i.e., 0.65/(1.0–0.01) × 0.75), assuming the change in the pK value is proportional to the change of ionic strength. We thus used 0.49 as the maximum uncertainty in pK values of organic acid charge groups due to ignoring ionic strength in the uncertainty analysis (see Section 2.4).

2.4. Evaluation of the effects of OrgAlk on the CO_2 system

The effect of OrgAlk on the CO_2 system was evaluated by incorporating OrgAlk expressions, including the equilibrium constants of all identified organic acid charge groups and total concentration of each charge group, into the

CO2SYS calculation program (van Heuven et al., 2011) as follows:

$$\mathrm{OrgAlk} = \sum_i \frac{X_{iT}}{1 + \frac{[H^+]}{K_i}} \quad (3)$$

Dissociation constants of carbonic acid, boric acid, HSO_4^-, and hydrogen fluoride were taken from Cai and Wang (1998), Dickson (1990a), Dickson (1990b), and Dickson and Riley (1979), respectively. The total boric acid concentration was computed from the equation of Lee et al. (2010). Measured values of TA, DIC, equilibrium constants and total concentrations of organic acid charge groups were used as input parameters to the CO2SYS program to calculate the values of H^+, pCO_2, and other CO_2 system parameters; the same calculation was then repeated, but with the total concentrations of organic acid charge groups set to zero. The effects of OrgAlk were then estimated as the differences in H^+ concentrations (ΔH^+), pCO_2 (ΔpCO_2), and other CO_2 parameters between the two calculations.

In the above calculations, TA and DIC values were fixed while OrgAlk varied. This is analogous to assuming that all organic acid charge groups are produced by organic acids, thus their variations will ultimately not change TA (Kuliński et al., 2014), since their dissociation leads to the production of an equivalent amount of H^+. Nevertheless, some organic acid charge groups might be produced concurrently with other cations (e.g., Ca^{2+}, Cu^{2+}, and Na^+) to maintain charge balance. For example, organic acid charge groups may cycle with Zn^{2+} or Cu^{2+} during dissociation/association of metal-humic complexes (Garcia-Mina, 2006; Shi et al., 2016), resulting in net gain or loss of TA. Given that there is little knowledge of how organic acid charge groups cycle with H^+ vs. with other cations, we do not know the exact magnitude of TA change when organic acid charge groups vary. This prevents us from resolving the CO_2 system without proper constraints on TA. Thus, we calculated the impact of OrgAlk by assuming no change in TA. The explicit calculation of the OrgAlk effects on the CO_2 system requires future studies on how these charge groups are generated and cycled in the aquatic environment. In our scenario (constant TA), OrgAlk does not have a direct effect on the carbonate alkalinity, but the variation in OrgAlk changes the H^+ concentration and, thus, affects carbonate alkalinity.

Buffer capacity is a measure of the resistance of a natural water or solution to pH change following the addition of an acid or base (Morel and Hering, 1993). The traditional buffer factor (β_H) can be calculated directly from the buffer factor (β_{Alk}) proposed by Egleston et al. (2010). Organic acid charge groups also provide buffer capacity and affect water pH and acid-base speciation, thus OrgAlk was added into the buffer capacity equation:

$$\beta_H = -\left(\frac{\partial \mathrm{pH}}{\partial \mathrm{TA}}\right)^{-1} = -2.3\beta_{Alk} \quad (4)$$

where

$$\beta_{Alk} = \frac{Alk_c^2}{DIC} - S \quad (5)$$

$$S = \sum_i \frac{[H^+][X_i^-]}{K_i + [H^+]} + \frac{[H^+][B(OH)_4^-]}{K_B + [H^+]} + [HCO_3^-] + 4[CO_3^{2-}] + [H^+] - [OH^-] \quad (6)$$

Alk_c and X_i^- represent the carbonate alkalinity and organic acid charge group i, respectively. The effect of OrgAlk on the buffer capacity was calculated as the difference between the buffer capacity calculated with and without OrgAlk ($\Delta\beta_H$). Note that the change of pH and acid-base speciation induced by OrgAlk could also affect the carbonate, borate, and other buffer systems in natural water. $\Delta\beta_H$ thus includes a direct effect of OrgAlk on β_H by offering extra buffer capacity and an indirect effect by influencing water pH and other buffer systems.

The uncertainties of OrgAlk effects on the H^+ concentration and pCO_2 were calculated using the error propagation program of Orr et al. (2018), modified by adding uncertainties in the estimated pK values of organic acid charge groups due to the effect of ionic strength. The uncertainties in $\Delta\beta_H$ were calculated based on a first-order Taylor series expansion, accounting for parameter uncertainties derived from the error propagation program and measurement uncertainties. The combined uncertainties in ΔH^+, ΔpCO_2, and $\Delta\beta_H$ include the uncertainties in pK values of organic acid charge groups, carbonic and boric acids, as well as DIC, TA, and OrgAlk measurement uncertainties.

3. RESULTS

3.1. Excess alkalinity versus titrated OrgAlk

Excess alkalinity (ΔTA), defined as the difference between measured TA and calculated TA using measured DIC and pH as input parameters in CO2SYS, has been used in the past to estimate OrgAlk (e.g., Kuliński et al., 2014; Yang et al., 2015; Ko et al., 2016; Hammer et al., 2017). In our analysis, pooled titrated OrgAlk and ΔTA data did not show a strong statistical relationship (Fig. 3). This may be due to colored material and fine particles (< 0.45 μm) in tidal water that interfere with spectrophotometric pH measurements. Nevertheless, in October and November, ΔTA and OrgAlk values were similar (mean ΔTA: 32 ± 8 μmol kg^{-1}, mean OrgAlk: 34 ± 7 μmol kg^{-1}) with the linear slope close to 1, compared to May (slope $\ll 1$) and July (slope < 1) when more water color and fine particles were observed in the samples (Fig. 3). Uncertainties in carbonate system calculations, including those in TA and DIC measurements and the dissociation constants of carbonic acid (Cai and Wang, 1998), boric acid (Dickson, 1990a), HSO_4^- (Dickson, 1990b), and hydrogen fluoride (Dickson and Riley, 1979), might also contribute to this discrepancy. Further studies are required to examine this difference, which also highlights the importance of directly measuring OrgAlk.

3.2. Tidal and seasonal variability

OrgAlk, DOC, TA, pH (total proton concentration scale at in-situ temperature), salinity, and temperature (T) in the Sage Lot Pond tidal creek in May, July, October,

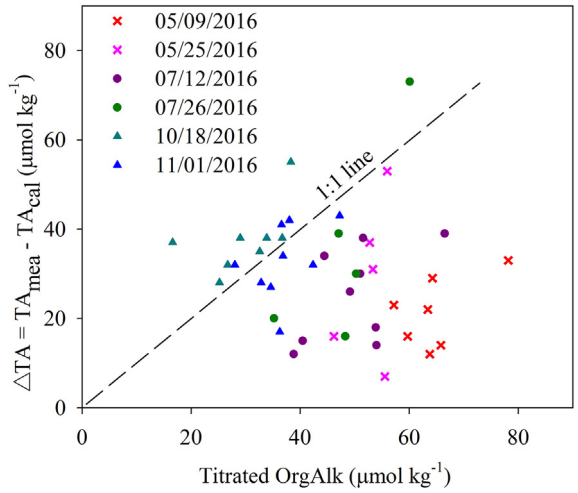

Fig. 3. Comparison between titrated OrgAlk concentrations and excess alkalinity (ΔTA) calculated as the difference between measured TA (TAmea) and calculated TA (TAcal) using measured DIC-pH as the input pair at Sage Lot Pond in May, July, October, and November 2016. The dashed line is a 1:1 line indicating where titrated OrgAlk concentrations are equal to excess alkalinity.

and November varied over tidal cycles and across all seasons (Fig. 4). pH was generally highest at high tide and lowest at low tide. Salinity typically varied by < 3 over a tidal cycle. DOC and OrgAlk showed similar trends over tidal cycles, with concentrations increasing from high to low tide.

In May, the salinity in the salt marsh tidal creek ($S_P = 22.5–29.0$, Fig. 4a and 4b) was much lower than in the adjacent coastal water ($S_P = \sim32$). This low salinity was due to GW input, since there is no river discharge at the study site. As such, three end-members (GW, salt marsh, and coastal water) may affect the carbonate chemistry in the tidal water at the study site. Salinity was higher on May 25th, suggesting a greater GW input on May 9th (Fig. 4a and b). On May 9th, the mean OrgAlk concentration was about 9 μmol kg^{-1} higher than on May 25th, but the mean TA value was about 180 μmol kg^{-1} lower (Fig. 4a and b). OrgAlk and DOC also covaried more strongly on May 9th (Fig. 4a).

In the summer, salinity was lower on July 12th ($S_P = 27.0–30.2$, Fig. 4c) than on July 26th ($S_P = 29.7–30.5$, Fig. 4d). In contrast to May, when TA did not show a clear covariation with tides, TA concentrations in July generally increased from high to low tide, especially on July 26th when TA increased > 100 μmol kg^{-1} (Fig. 4c and 4d). This is consistent with previous observations of TA production by anaerobic respiration in tidal marshes (Wang et al., 2016). DOC was up to 100 μmol kg^{-1} higher at low tide than at high tide in the summer, similar to the TA trend (Fig. 4c and d), indicating in-situ production of DOC in salt marshes. Interestingly, although DOC concentrations in July were generally higher than in May, OrgAlk concentrations were lower in July than in May when the influence of GW was apparent. Meanwhile, OrgAlk concentrations were elevated by 10–20 μmol kg^{-1} from high to low tide in July (Fig. 4c and d).

In October and November, the influence of GW was even more limited, with salinity > 28.8 (Fig. 4e and f). During the fall sampling events, average water elevation was higher than in spring or summer. TA varied from 1884 to 1998 μmol kg^{-1} over two tidal cycles, generally lower than in July (Fig. 4). Both DOC and OrgAlk concentrations were the lowest observed among the three seasons (Fig. 4).

3.3. Characteristics of organic acid charge groups

Apparent pK values and total concentrations of organic acid charge groups in GW, Vineyard Sound coastal water and tidal waters across three seasons were determined by fitting the non-linear model (Eq. (2)) to the full titration data (Table 1). As an example, the May 25th full titration of sample D is shown in Supplementary Data A2. The simulated concentration of CO_3^{2-} in NaOH solution was 1.2 mmol L^{-1} on average (range 0.5–1.5 mmol L^{-1}). The estimated pK values of the organic acid charge groups showed a 0.1–0.4 difference when calculated with and without the carbonate alkalinity from the NaOH solution. Two organic acid charge groups were identified in all titrated samples. The pK value of charge group 1 (pK_1) ranged from 4.1 to 5.5, with the highest value in sample B collected on May 9th, and the lowest value in sample D collected on May 25th. Most pK values of charge group 2 (pK_2) were in the range of 7.4–8.4, except sample A on May 9th with a much higher value of 9.8. Sample A was collected during the same time series as samples B and C at similar salinities (Table1). The pK values of the two charge groups in samples B (5.5 and 7.4) and C (5.1 and 7.8) were similar to those in the GW (4.9 and 7.6), which was consistent with the strong influence of the GW (Table 1). Given how different sample A is from all others, it appears likely that contamination or preservation issues might have occurred. Nevertheless, the pK values of sample A are listed for data completeness, but will not be used for further analysis or discussion. In tidal waters, the total concentrations of the two charge groups showed clear differences among seasons, with much higher values in summer, followed by autumn and spring (Table 1).

3.4. Effects of OrgAlk on the CO_2 system and buffer capacity

The impact of OrgAlk on the CO_2 system (i.e. ΔH^+, ΔpCO_2, and $\Delta\beta_H$ defined in Section 2.4) is shown as a function of relative OrgAlk abundance (OrgAlk% in TA) and measured pH (Fig. 5). Use of relative OrgAlk abundance, rather than concentration, accounts for tidal and seasonal changes of both OrgAlk and TA. Since full titrations were only conducted on one sample for each sampling date except May 9th and October 18th, we assume that all remaining samples from the same sampling event contain similar charge groups, with the same pK_1, pK_2, and total concentration ratios of the two charge groups (last column in Table 1 and Fig. 5). The mean pK_1 and pK_2 values and mean total concentration ratio of the two charge groups in samples B and C were used to calculate the effects on May 9th. The samples collected on October 18th were assumed to have the same organic acid charge group characteristics as

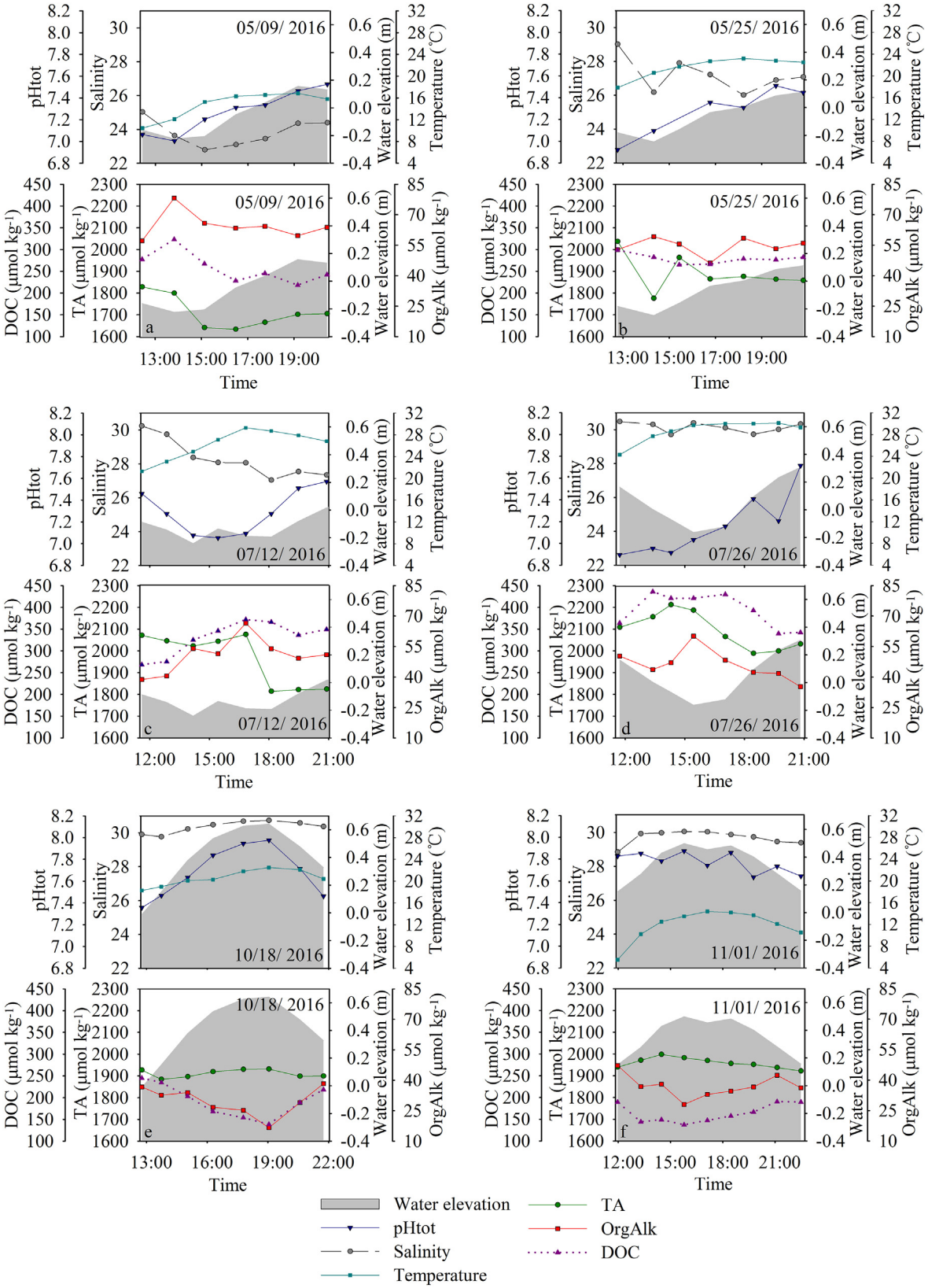

Fig. 4. Variations of TA, OrgAlk, pHtot (pH on the total proton concentration scale at in-situ temperature), salinity, DOC, temperature, and water elevation (NAVD88) over tidal cycles in May (a, b), July (c, d), October (e), and November (f) 2016 at Sage Lot Pond. The scales for each parameter are consistent across plots for convenience of comparison.

Table 1
Summary of full-titration of the samples collected in the study. pK_1 and pK_2 represent the modeled pK values of identified organic acid charge group 1 and charge group 2. X_{1T} and X_{2T} are the estimated total concentrations of charge group 1 and charge group 2, respectively. GW and VS represent groundwater and Vineyard Sound coastal water, respectively.

Sample	Collecting date	Salinity	pH	Titrated OrgAlk (μmol kg^{-1})	pK_1	pK_2	X_{1T} (μmol kg^{-1})	X_{2T} (μmol kg^{-1})	X_{2T}/X_{1T}
A	2016.5. 9	22.8	7.20	66	5.0	9.8	35	14	0.4
B	2016.5. 9	23.6	7.00	78	5.5	7.4	21	33	1.6
C	2016.5. 9	23.4	7.33	64	5.1	7.8	24	33	1.4
D	2016.5. 25	29.0	6.92	53	4.1	7.9	62	89	1.4
E	2016.7.12	27.0	7.28	54	4.4	8.1	100	258	2.6
F	2016.7.26	30.3	7.71	35	4.2	8.4	117	301	2.6
G	2016.11.1	28.8	7.83	47	4.6	8.4	104	236	2.3
GW	2016.9.16	0.5	6.66	435	4.9	7.6	221	316	1.4
VS	2018.7.9	32.0	7.87	16	4.9	8.3	36	92	2.6

those collected on November 1st. The total concentration of each charge group in any given sample was calculated using the titrated OrgAlk concentration, the pK values, and the total concentration ratio of the two charge groups from the full titration. The ranges of ΔH^+, ΔpCO_2, and $\Delta\beta_H$ observed in tidal waters were significant given the combined uncertainties in ΔH^+, ΔpCO_2, and $\Delta\beta_H$ (Fig. 5).

In general, the effects of OrgAlk on H^+ concentrations (ΔH^+) ranged from 1 to 41 nmol kg^{-1} (equivalent to a pH change of 0.03–0.26), increasing concurrently with the increasing OrgAlk% in TA across all three seasons at SLP (Fig. 5a). There was some seasonality in the effects of OrgAlk on H^+ concentrations as well. The largest effect was observed in May, coincident with the highest OrgAlk % in TA among the three seasons, subsequently decreasing in July, followed by October and November. The impact of OrgAlk on H^+ decreased consistently with increasing tidal water pH (Fig. 5b). In some July samples, OrgAlk increased H^+ concentrations considerably, but OrgAlk% in TA did not increase proportionately, highlighting that the effect of OrgAlk is influenced by both the relative OrgAlk abundance and water pH (Fig. 5a and b).

An increase of OrgAlk% in TA would generally increase pCO_2 in all three seasons, showing a similar pattern as ΔH^+ (Fig. 5). The OrgAlk effect on pCO_2 varied by 8–80% with a mean of 38% across the OrgAlk range (0.9–4.3% in TA) observed in this study. Relatively large effects on pCO_2 occurred in May (Fig. 5c), when the relative OrgAlk abundance was generally high and sample pH was low. ΔpCO_2 was lower in July (mean ~880 μatm) than in May (mean ~960 μatm) and reached the lowest values in October and November (mean ~200 μatm). ΔpCO_2 increased with a decrease in pH (Fig. 5d), as more carbonate species shifted to dissolved CO_2 at lower pH. The large variation of ΔpCO_2 over tidal cycles on May 25th and in July can be attributed to the large variation in pH (Fig. 5d). Compared to October and November, the higher ΔpCO_2 values at similar OrgAlk% in July may also be due to lower pH values (Fig. 5c and d).

Compared with H^+ and pCO_2, the effect of OrgAlk on the buffer capacity ($\Delta\beta_H$) was more complex (Fig. 5e and f). As the proportion of OrgAlk in TA increased, its effect on β_H generally changed from reducing buffer capacity (negative values) to increasing buffer capacity (positive values), and in many cases the effect was close to zero. In July and on May 25th, $\Delta\beta_H$ showed both positive and negative values over the same tidal cycle, while on May 9th, OrgAlk effects were generally positive, compared with the mainly negative values in October and November. Similar to ΔpCO_2, some samples over the same tidal cycle at similar OrgAlk% showed large variations in $\Delta\beta_H$, especially on May 25th and July 12th. Such an effect can be better illustrated in the $\Delta\beta_H$–pH plot (Fig. 5f), where there was generally a negative relationship with pH (Fig. 5f). When pH was below ~7.5, $\Delta\beta_H$ was generally positive, while when pH was > 7.5, $\Delta\beta_H$ became negative. This is coincident with the minimum buffer capacity of seawater occurring at pH ≈ 7.5. When pH is > 7.5, CO_3^{2-} provides the main control on the buffer capacity, while when pH is < 7.5, HCO_3^- is the principal species in control. As a result, there is a relatively large scatter in $\Delta\beta_H$ at similar OrgAlk%, depending on sample pH (Fig. 5e).

4. DISCUSSION

4.1. Sources of OrgAlk

Tidal creeks within salt marshes are mixing zones between coastal water, GW, and porewater flushed from the marsh during tidal exchange. Mixing of these three sources was apparent during all three seasons (Fig. 6). The coastal water OrgAlk concentration was generally lower than in waters from the salt marsh tidal creek (Fig. 6). Although coastal waters were not sampled on the same dates as the salt marsh tidal creek, we anticipate the seasonal and interannual variation of OrgAlk in Vineyard Sound to be small, given that OrgAlk concentrations in March and July were similarly low (21 and 16 μmol kg^{-1}, respectively) (Fig. 6). Within the tidal creek, OrgAlk concentrations increased as salinity decreased although there were considerable variations among both tidal cycles and seasons. This suggests that GW, as the main freshwater source, may be an important source of OrgAlk to the marsh-influenced tidal water.

The salt marsh is likely another significant OrgAlk source. The highest DOC concentrations in tidal waters

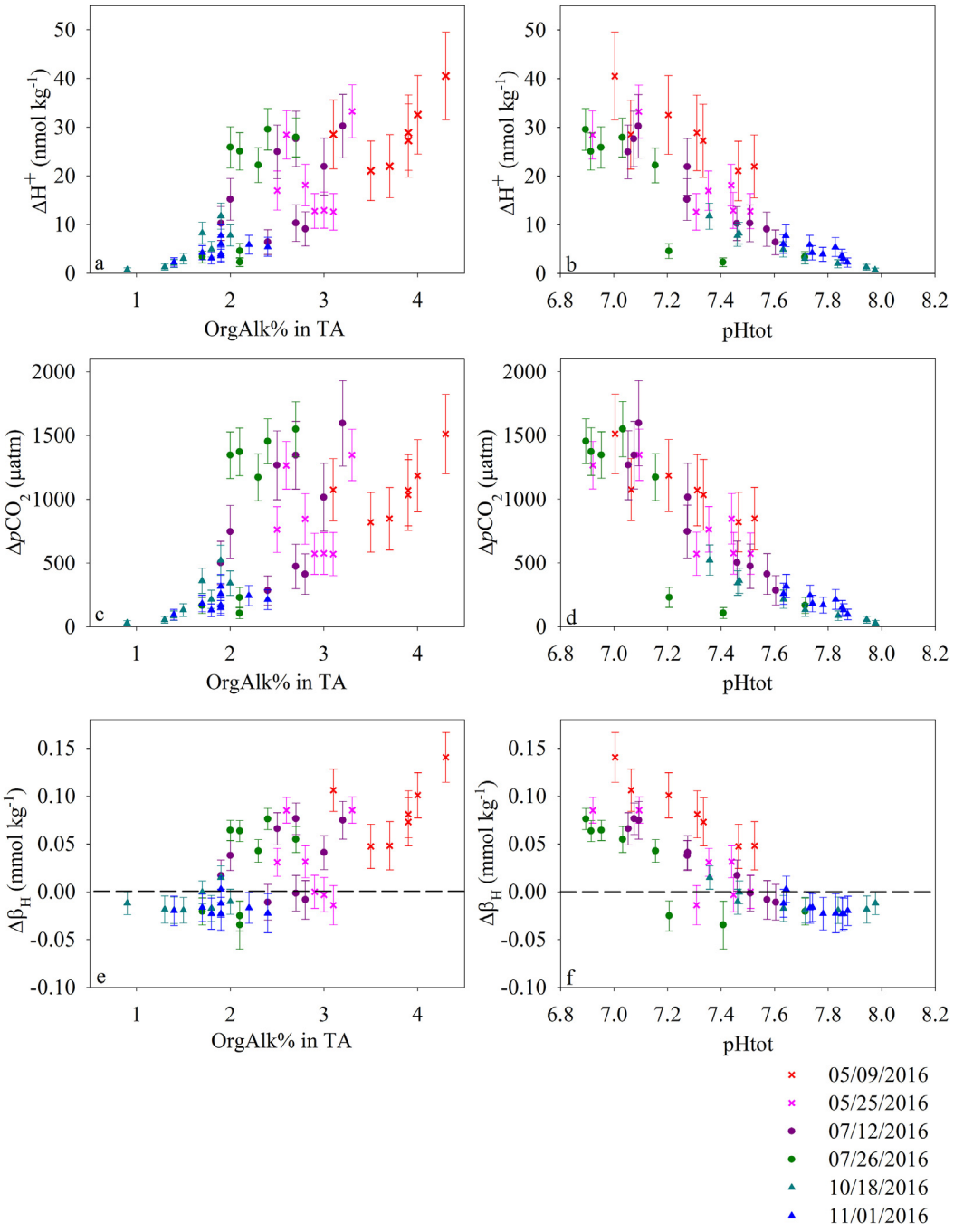

Fig. 5. The effects of OrgAlk on H^+, pCO_2, and buffer capacity (β_H) over three seasons at Sage Lot Pond. ΔH^+, ΔpCO_2, and $\Delta\beta_H$ represent the differences in H^+, pCO_2, and β_H between the values calculated by including OrgAlk and those without, using measured TA and DIC as input pair. (a), (c), and (e) show ΔH^+, ΔpCO_2, and $\Delta\beta_H$ variations with OrgAlk% in TA in May, July, October, and November 2016. (b), (d), and (f) show the changes of ΔH^+, ΔpCO_2, and $\Delta\beta_H$ as a function of measured pH. The vertical bars for data points indicate the uncertainties in ΔH^+, ΔpCO_2, and $\Delta\beta_H$, respectively.

appeared in July when the GW influence was relatively low (Fig. 4), implying high in-situ production in the salt marsh. OrgAlk concentrations generally increased with increasing DOC concentrations during the period of low GW influence (July 26th, October, and November) (Fig. 7), an indication of OrgAlk contribution from the marsh.

The relative contributions of GW and marsh production to OrgAlk were assessed based on conservative mixing between the GW and coastal water end-members, and OrgAlk additions in tidal waters. The three GW samples collected from different depths were variable (177–485 μmol kg^{-1}). If the GW sample collected at shallow

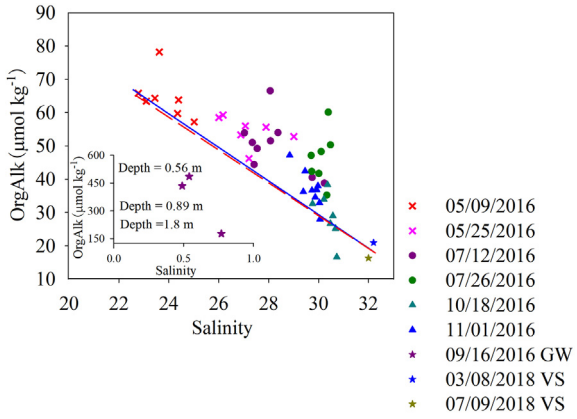

Fig. 6. Variations of OrgAlk concentrations with salinity in tidal water at Sage Lot Pond (SLP) in May, July, October, and November 2016. The purple stars in the inset represent OrgAlk concentrations in GW collected at the edge of the SLP marsh (41.55443N, 70.5054W; Fig. 1). The yellow and blue stars at high salinity represent OrgAlk concentrations in coastal water of Vineyard Sound (VS) off SLP. The dashed red line is the mixing line between Vineyard Sound water and GW at depth of 1.8 m. The solid blue line is the mixing line between Vineyard Sound water and the lowest salinity SLP tidal water. (For interpretation of the references to color in this figure legend, the reader is referred to the web version of this article.)

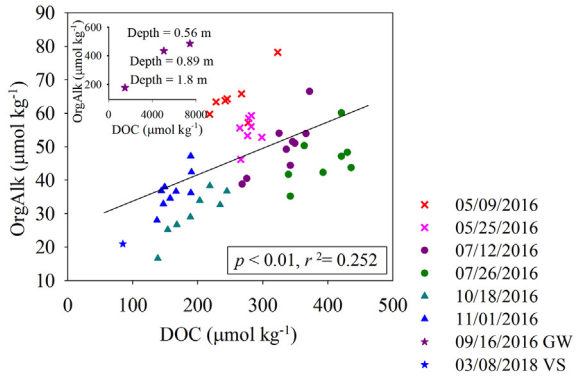

Fig. 7. Variations of OrgAlk and DOC concentrations in tidal creek water at SLP in May, July, October, and November 2016. The purple stars in the inset show OrgAlk and DOC concentrations in GW collected at the edge of the SLP marsh. The blue star represents OrgAlk and DOC concentrations in Vineyard Sound coastal water (VS) off SLP. The black line indicates the linear correlation between DOC and OrgAlk concentrations ($p < 0.01$, $r^2 = 0.252$, $n = 48$). (For interpretation of the references to color in this figure legend, the reader is referred to the web version of this article.)

depth (485 μmol kg^{-1}, 0.56 m) represented the potential GW end-member, then the tidal creek samples would fall below the mixing line between GW and Vineyard Sound waters, implying that the marsh is a significant OrgAlk sink. The marsh was a pronounced source of DOC (Fig. 4), so such an explanation is unlikely. The deep GW (177 μmol kg^{-1}, 1.8 m) may be a more reasonable end-member. Indeed, the mixing line connecting the average values of the two Vineyard Sound waters with the GW collected at 1.8 m (dashed red line in Fig. 6) is similar to the mixing line between Vineyard Sound water and the lowest salinity tidal water sample (solid blue line in Fig. 6). The extrapolated freshwater end-member of this tidal water mixing line was 182 μmol kg^{-1}, similar to the deep GW. Therefore, we considered the deep GW as the most representative freshwater end-member to constrain the GW OrgAlk contribution to tidal water, recognizing that the best end-member would be a flow-weighted average of GW discharging to the creek.

The potential GW OrgAlk contributions to tidal creek samples were calculated from sample salinity, assuming conservative mixing between coastal water and the deepest GW, while marsh contributions were assessed based on deviations above this mixing line (dashed red line in Fig. 6). Over tidal cycles in May and on July 12th when the GW influence was high, GW contributed, on average, 54% of the measured OrgAlk, much more than the average marsh contribution of 17%. In tidal water samples with limited GW influence (July 26th, October, and November), the marsh contribution accounted for 0–54% of OrgAlk concentrations with a mean value of 20%, compared to an average GW contribution of 31%. The greatest marsh contribution occurred on July 26th, when an estimated mean of 36% of the OrgAlk in tidal water was from the marsh, greater than the GW contribution with a mean of 24%. We further note that the concentration analysis provided here does not consider varying water flux rates across tidal cycles and variability of the GW source, which may cause potential uncertainties in this analysis.

4.2. Variations of OrgAlk versus DOC

OrgAlk showed a generally positive correlation ($p < 0.01$, $r^2 = 0.252$, $n = 48$) with DOC in tidal creek water (Fig. 7). Nevertheless, it is apparent that some non-OrgAlk molecules in the DOC pool cycled differently from organic acid charge groups. Whereas OrgAlk samples fell along or above the conservative mixing line between deep GW and Vineyard Sound coastal water (Fig. 6), almost all of the tidal creek DOC samples in May fell below it (Supplementary Data A3). It is likely that humic substances, which may be the main components of OrgAlk (Cai et al., 1998; Lukawska-Matuszewska et al., 2018), are relatively recalcitrant and thus preferentially preserved, relative to other organic molecules in the DOC pool, during GW transport and water mixing within the tidal creek.

The complex relationship between OrgAlk and DOC can be evaluated through OrgAlk:DOC ratios in tidal waters, GW, and Vineyard Sound coastal waters over different tides and seasons (Fig. 8). The GW samples contained high OrgAlk concentrations (Fig. 6) and very high DOC concentrations (1500 μmol kg^{-1} in deep GW to 7000 μmol kg^{-1} in shallow GW), which resulted in extremely low OrgAlk:DOC ratios (< 0.15). The OrgAlk:DOC ratio increased with GW depth, accompanied with a three-fold OrgAlk decrease vs. a five-fold DOC decrease, which may again indicate preferential removal of some non-OrgAlk components of the DOC pool relative to organic acid charge groups along the GW flow path. In

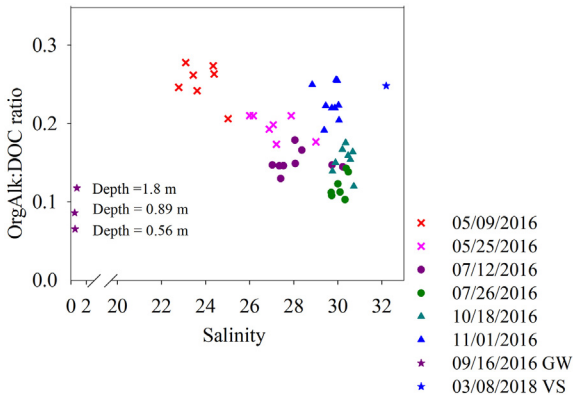

Fig. 8. Variations of OrgAlk:DOC ratios with salinity in tidal water at Sage Lot Pond in May, July, October, and November 2016, and in GW and Vineyard Sound coastal water end-members.

the tidal creek, OrgAlk:DOC ratios were highest in May among the three sampling seasons, when the GW influence was greatest (Fig. 8). Since GW has a low OrgAlk:DOC ratio, the plausible explanation again might be of the preferential removal of non-OrgAlk molecules in the DOC pool during GW transport and water mixing within the tidal creek. The OrgAlk:DOC ratios were lowest in July, concurrent with much higher DOC, relative to OrgAlk production in the salt marsh (Fig. 7). Coastal water and the tidal waters in October and November showed relatively high OrgAlk:DOC ratios, driven by low DOC concentrations.

Previous studies have used fixed organic acid to DOC ratios to estimate the abundance of OrgAlk from DOC concentrations (e.g., Morel and Hering, 1993; Hunt et al., 2011; Wang et al., 2013). Furthermore, recent studies have tried to determine the acid-base properties of DOC using a single acid-base dissociation constant and a fixed fraction of DOC (Kuliński et al., 2014; Ulfsbo et al., 2015; Hammer et al., 2017). The results from this study suggest that the OrgAlk:DOC ratio is highly variable over both time (tidal and seasonal cycle, 0.1–0.28) and space (GW, marsh tidal and coastal waters, 0.07–0.28), potentially driven by various controlling factors such as DOC sources and quality, water mixing, and decomposition processes. This work as well as previous studies suggest that the sources of organic acid charge groups in coastal water include rivers, wetlands, groundwater, and phytoplankton production, all of which respond to different environmental drivers, thus altering OrgAlk:DOC ratios. Therefore, it is insufficient to account for OrgAlk contributions through DOC concentration measurements alone.

4.3. Characteristics of identified charge groups

The apparent pK values of organic acid charge groups were used to identify the characteristics of these charge groups. The first charge group had a pK_1 value of 4.1–5.5 (Table 1), and likely corresponds to the carboxylic acid group (Cai et al., 1998). The carboxylic acid group is present in coastal waters and culture experiments of marine phytoplankton (Muller and Bleie, 2008; Ko et al., 2016), and considered to be a significant contributor to alkalinity in natural waters (Ritchie and Perdue, 2003). GW had a pK_1 value (4.9) similar to Vineyard Sound coastal water (4.9), suggesting an analogous carboxylic acid group composition. The pK_1 values in the tidal creek samples with low salinity (Sp = 23–24, pK_1 = 5.1–5.5) were close to that in GW, consistent with a GW source of OrgAlk in the tidal creek. In tidal water samples with higher salinity (Sp = 27–31), pK_1 values (4.1–4.6) were lower than those in the two end-members, potentially indicating influence of marsh pore water.

The 2nd charge group had a pK_2 value of 7.4–8.4 (Table 1) and may match phenolic or amine species, as reported by Paxeus and Wedborg (1985) in river samples with pK = 8.11. Compared to GW (pK_2 = 7.6), Vineyard Sound coastal water had a higher pK_2 value (8.3), suggesting disparate phenolic or amine species in these waters. The pK_2 values in samples B (7.4) and C (7.8) with low salinity (Sp = 23–24) were similar to that in GW, while the samples collected in July and November had pK_2 values (8.1–8.4) similar to Vineyard Sound coastal water. Thus, the characteristics of the charge groups reflect significant GW influence in the tidal creek in May, but greater contributions from both coastal water and marsh sources in July and November. The tidal creek water contained more phenolic and/or amine species than carboxylic acid groups, as shown by the higher total concentrations of X_{2T} than X_{1T} (Table 1). Nonetheless, charge group 1 contributed more to TA in all seasons due to its much lower pK values, resulting in more deprotonated carboxylic acid groups in the pH range of marsh tidal water. Note that the concentration of OrgAlk should theoretically be equal to the sum of $[X_1^-]$ + $[X_2^-]$ (not the sum of $X_{1T} + X_{2T}$, since these contain both the acid and base pairs). Nevertheless, the estimated $[X_1^-]$ and $[X_2^-]$ for these samples did not exactly match titrated OrgAlk concentrations, likely because we ignored the effects of ionic strength when we modeled the organic acid charge groups.

It is worth noting that Ulfsbo et al. (2015) proposed that OrgAlk might not fit well with Dickson's definition of TA (Dickson, 1981). Dickson chose a pH endpoint of 4.5, far from the pK values of the main weak acids in seawater (i.e., carbonic acid, boric acid, sulfate, etc.), so that the dissociation-association reactions of these acids are complete at the pH endpoint. However, these results and previous studies (Cai et al., 1998; Muller and Bleie, 2008; Ulfsbo et al., 2015) indicate that some organic acid charge groups might have pK values near 4.5, making acid-base categorization difficult for them. In addition, the traditional Gran-type titration method used here and in many other studies is conducted in the pH range of 3.0–3.8. Some organic acid charge groups may be titrated in this lower pH range that would not otherwise be titrated at pH 4.5, thus causing potential bias in OrgAlk concentrations, based on the definition of TA. Nevertheless, given the uncertainty in the pK values of these organic charge groups, we cannot predict whether titrated OrgAlk is biased and by how much. Future studies are warranted to address how to better include OrgAlk in the TA definition and to improve titration methods to determine OrgAlk more accurately.

4.4. Common effects of OrgAlk in different coastal waters

Given the similarity in charge groups of organic acids in coastal waters across multiple seasons and different environments, as shown in this study (Section 4.3) and others, we examined whether there are any common features or differences in OrgAlk effects on carbonate chemistry across various coastal water systems. Here, we define coastal systems as the area from the upper reach of tidal water to the shelf break. We consider three idealized environments that represent typical scenarios in the northeastern U.S. coastal region: (1) offshore coastal water, (2) marsh-influenced water without any freshwater input, and (3) estuarine water, where offshore coastal water mixes with a freshwater source rich in OrgAlk, such as river water or GW. In each case, the characteristics of salinity, temperature, TA, DIC, and OrgAlk were set at representative values of these coastal environments as observed in this study (Table 2). The effects of OrgAlk on the CO_2 system speciation and buffer capacity (ΔH^+, ΔpCO_2, and $\Delta\beta_H$) were estimated as discussed in Section 3.4 by varying X_{1T} and X_{2T} concentrations, thus changing OrgAlk% in TA, but keeping the X_{2T}/X_{1T} and pK values of charge groups constant (Fig. 9).

For all three cases, as the OrgAlk relative contribution to TA increases, its effect on the H^+ concentration increases (Fig. 9a), while the magnitude is somewhat different for each case. Marsh-influenced water (case 2) shows the greatest sensitivity to increasing proportion of OrgAlk, followed by estuarine water (case 3) and offshore coastal water (case 1). The main reason for the different sensitivity of ΔH^+ to OrgAlk% in TA are the specific DIC and TA conditions of each of the three cases that result in different water pH and buffer capacity. Compared to offshore coastal water, estuarine water and marsh-influenced water have lower buffer capacities, as their initial pH values are near 7.5. Lower pH in marsh-influenced water leads to a greater change in H^+ concentration with OrgAlk addition, compared to the other two cases. Nevertheless, the magnitude of the effect of OrgAlk on H^+ concentration is significant for all three

Table 2
Input parameters and OrgAlk characteristics used in CO2SYS calculations in three coastal water environments. The OrgAlk characteristics in offshore coastal water and marsh-influenced water were similar to the Vineyard Sound water sample and the low pH sample D in Table 1, respectively. The OrgAlk characteristic in estuarine water was based on the mean pK_1, pK_2, and X_{2T}/X_{1T} values between samples B and C in Table 1.

	Salinity	Temperature (°C)	TA (μmol kg^{-1})	DIC (μmol kg^{-1})	pK_1	pK_2	X_{2T}/X_{1T}
Offshore coastal water	32.0	10	2100	1950	4.9	8.3	2.6
Marsh-influenced water	32.0	10	2200	2300	4.1	7.9	1.4
Estuarine water	20	10	1320	1360	5.2	7.6	1.5

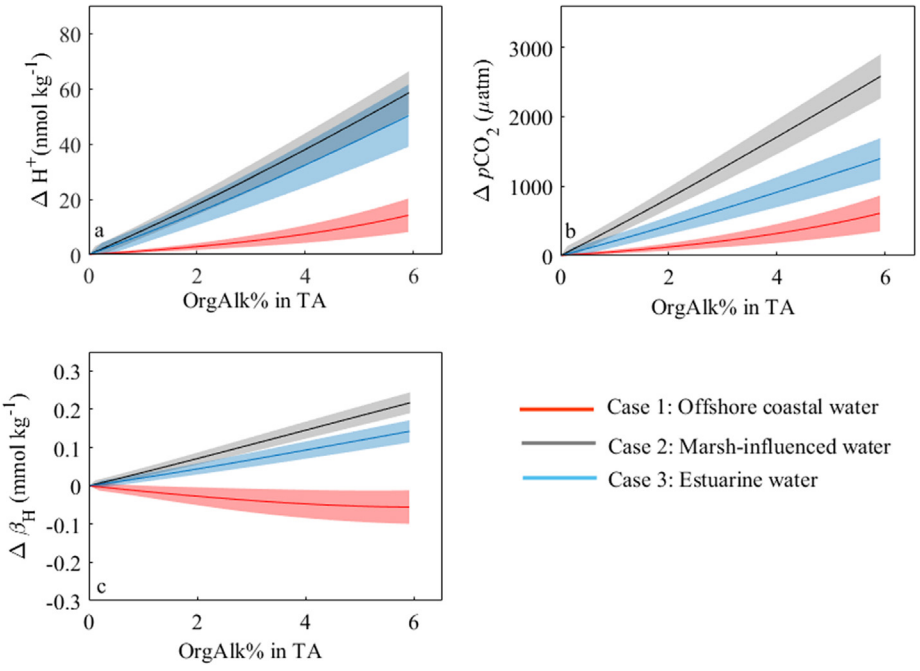

Fig. 9. Effects of OrgAlk on H^+ (a), pCO_2 (b), and β_H (c) in three cases of coastal waters. ΔH^+, ΔpCO_2, and $\Delta\beta_H$ were calculated similarly as in Fig. 5 (also see Section 3.4). The color bands around each solid line of three cases of coastal waters indicate the uncertainties in ΔH^+, ΔpCO_2, and $\Delta\beta_H$. (For interpretation of the references to color in this figure legend, the reader is referred to the web version of this article.)

cases of coastal environments, with the largest H^+ concentration increase of 8–41 nmol kg^{-1} (equivalent to a pH change of 0.23–0.27) in the OrgAlk proportion range (0.9–4.3%) observed in this study.

Similar to H^+ concentration, the impact of OrgAlk on pCO_2 increases with the relative abundance of OrgAlk in the three coastal waters (Fig. 9b). The impact on pCO_2 is more pronounced for marsh-influenced water and estuarine water than for offshore coastal water mainly because of the difference in their buffer capacity. Dissolved CO_2, thus pCO_2, of offshore coastal water increases slowly as a result of CO_3^{2-} buffering until most of CO_3^{2-} is consumed and the water shifts to a HCO_3^- buffer system (Fig. 9b). In contrast, both marsh-influenced water and estuarine water have an initial pH near 7.5, so less CO_3^{2-} exists to buffer against increased dissolved CO_2 in the system. Therefore, in the more acidic coastal environments, such as tidal marshes and freshwater-influenced estuaries, the effect of OrgAlk on pCO_2, and thus CO_2 fluxes, is expected to be greater than in offshore water. It is worth noting that OrgAlk influences pCO_2 values by changing water pH thus the speciation of carbonic acid in natural waters. Using measured pH and DIC as the input pair to calculate pCO_2 values accounts for the effect of OrgAlk, resulting in a much smaller pCO_2 calculation error. Using pH and TA as the input pair, without correcting the latter for OrgAlk, is equivalent to treating OrgAlk as carbonate alkalinity in TA. This will overestimate DIC and pCO_2 values in carbonic acid speciation calculations. Lastly, using the TA-DIC pair without accounting for OrgAlk will result in underestimation of pCO_2 values, as shown in this study.

OrgAlk affects β_H for the three coastal water cases, similarly to pCO_2 (Fig. 9c). As the relative OrgAlk proportion increases in offshore coastal waters, lowering pH, β_H decreases (i.e., negative $\Delta\beta_H$) until pH decreases to ~7.5 (the case 1 curve becomes flat in Fig. 9c). On the other hand, both marsh and estuarine waters are already HCO_3^- buffer systems, and thus increasing OrgAlk% increases HCO_3^- concentration, and thus β_H (positive $\Delta\beta_H$).

5. A CONCEPTUAL COASTAL ORGALK MODEL

This study has systematically investigated the contributions of organic acid charge groups in the DOC pool to TA and estimated the impact of OrgAlk on the CO_2 system in salt marsh- and groundwater-influenced coastal water for the first time. The high concentrations of OrgAlk observed in marsh tidal water have an important effect on water pH, carbonate speciation, and thus CO_2 fluxes. To summarize, we present a conceptual model of OrgAlk sources and sinks within the coastal ocean (Fig. 10) based on the findings from this and previous studies (Kieber et al., 1990; Lovley

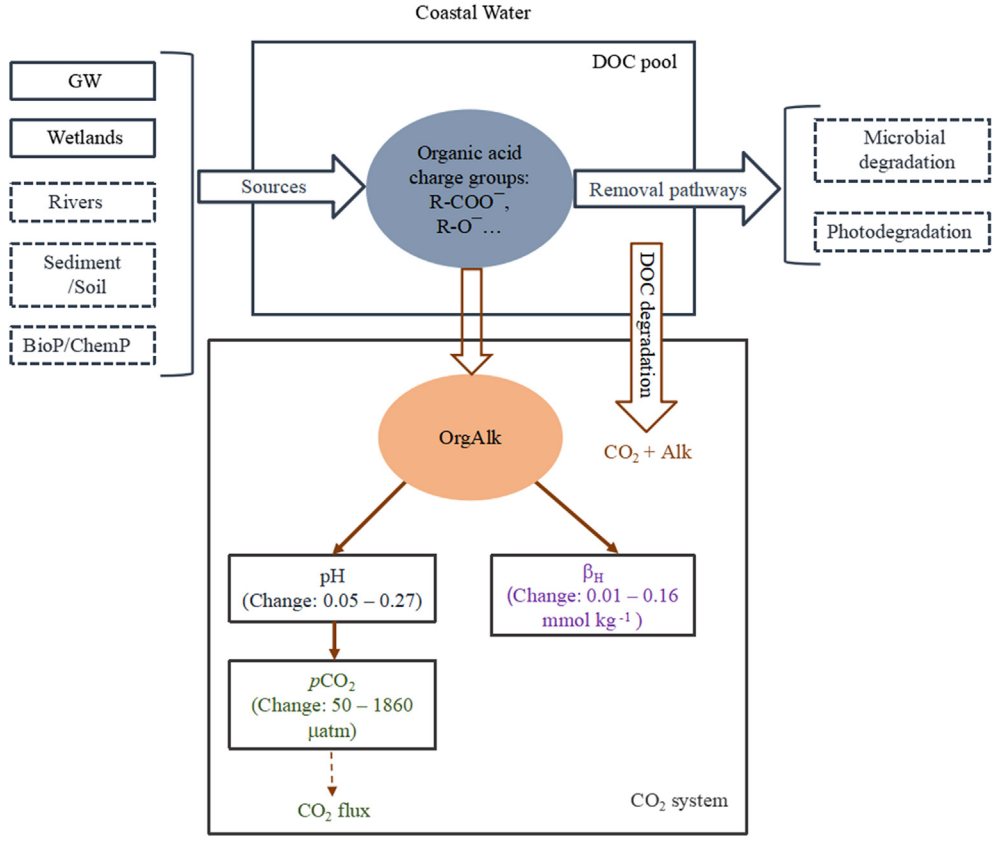

Fig. 10. A conceptual model of OrgAlk cycling in coastal systems. Alk indicates alkalinity. BioP and ChemP represent in-situ biological production and chemical production of organic acid charge groups, respectively. Boxes with dashed lines indicate processes that were not studied in the present study. The values in the boxes of pH, pCO_2, and buffer capacity (β_H) represent the magnitude of OrgAlk effects on pH, pCO_2, and β_H in the range of OrgAlk% in TA observed in this study (0.9–4.3%) in coastal waters.

et al., 1996; Cai et al., 1998; Uyguner and Bekbolet, 2005; Hernández-Ayon et al., 2007; Muller and Bleie, 2008; Kim and Lee, 2009; Wang et al., 2013; Ko et al., 2016; Hammer et al., 2017; Lukawska-Matuszewska et al., 2018). Traditionally, DOC contributes to the DIC pool through microbial remineralization, generating CO_2 and alkalinity (mostly by anaerobic pathways), and by photodegradation. In the conceptual model shown here, the organic acid charge groups of the DOC pool directly contribute alkalinity (OrgAlk), providing a biogeochemical link between the DOC and DIC pools in the coastal ocean by partially regulating pH, and thus pCO_2 and buffer capacity (Fig. 10).

In coastal environments where OrgAlk concentrations may be high, it is important to consider the effect of OrgAlk on the CO_2 system and carbon fluxes. As the composition of organic acid charge groups are inherently complex, the modeling method used in this and other studies (i.e. Eq. (2)) still lacks the ability to discern charge groups of organic acids across coastal waters with different ionic strengths. The model by Ulfsbo et al. (2015) might facilitate explicit understanding of the composition of organic acid charge groups in marine environments since it combines a humic ion binding model with an ionic interaction model. In general, we have a limited understanding of the generation and removal pathways of organic acid charge groups, their composition, and biogeochemical role in coastal waters and beyond. Thus, future studies are warranted to improve our understanding of organic acid charge groups in order to better quantify the linkage between organic and inorganic carbon cycling.

RESEARCH DATA

The data associated with this article can be accessed at https://www.bco-dmo.org/dataset/794163 (https://doi.org/10.1575/1912/bco-dmo.794163.1).

Declaration of Competing Interest

The authors declare that they have no known competing financial interests or personal relationships that could have appeared to influence the work reported in this paper.

ACKNOWLEDGEMENTS

We thank the associate editor Alfonso Mucci and three anonymous reviewers for their insightful comments, which improved the manuscript significantly. We thank Kate Morkeski, Lloyd Anderson, Zoe Sandwith, Xiao-bo Ni, Mallory Ringham, Eyal Wurgaft, Wei-jun Cai, Wen-yun Guo, and Ai-mei Wang for sampling, analytical, and modeling assistance; USGS staff including T. Wallace Brooks, Jennifer O'Keefe Suttles, Adrian Mann for field and analytical support; Jordan Mora and other staff at the Waquoit Bay NERR for sampling, analysis, and mapping support. The study was supported by the USGS Coastal & Marine Geology Program, the USGS Land Change Science Program's LandCarbon program, the U.S. National Science Foundation (OCE-1459521), the NOAA Science Collaborative program (NA09NOS4190153), and the China Scholarship Council. Any use of trade, firm or product names is for descriptive purposes only and does not imply endorsement by the U.S. Government.

APPENDIX A. SUPPLEMENTARY MATERIAL

Supplementary data to this article can be found online at https://doi.org/10.1016/j.gca.2020.02.013.

REFERENCES

Abril G., Bouillon S., Darchambeau F., Teodoru C. R., Marwick T. R., Tamooh F., Ochieng O. F., Geeraert N., Deirmendjian L., Polsenaere P. and Borges A. V. (2015) Technical Note: Large overestimation of pCO_2 calculated from pH and alkalinity in acidic, organic-rich freshwaters. *Biogeosciences* **12**, 67–78.

Bauer J. E., Cai W. J., Raymond P. A., Bianchi T. S., Hopkinson C. S. and Regnier P. A. G. (2013) The changing carbon cycle of the coastal ocean. *Nature* **504**, 61–70.

Butman D. and Raymond P. A. (2011) Significant efflux of carbon dioxide from streams and rivers in the United States. *Nature Geosci.* **4**, 839–842.

Cai W. J. (2011) Estuarine and coastal ocean carbon paradox: CO_2 sinks or sites of terrestrial carbon incineration? *Ann. Rev. Mar. Sci.* **3**, 123–145.

Cai W. J. and Wang Y. (1998) The chemistry, fluxes, and sources of carbon dioxide in the estuarine waters of the Satilla and Altamaha Rivers, Georgia. *Limnol. Oceanogr.* **43**, 657–668.

Cai W. J., Wang Y. and Hodson R. E. (1998) Acid-base properties of dissolved organic matter in the estuarine waters of Georgia, USA. *Geochim. Cosmochim. Acta* **62**, 473–483.

Cambareri T. C. and Eichner E. M. (1998) Watershed delineation and ground water discharge to a coastal embayment. *Groundwater* **36**, 626–634.

Chu S. N., Wang Z. A., Gonneea M. E., Kroeger K. D. and Ganju N. K. (2018) Deciphering the dynamics of inorganic carbon export from intertidal salt marshes using high-frequency measurements. *Mar. Chem.* **206**, 7–18.

Dickson A. G. (1981) An exact definition of total alkalinity and a procedure for the estimation of alkalinity and total inorganic carbon from titration data. *Deep Sea Res. Part A. Oceanogr. Res. Pap.* **28**, 609–623.

Dickson A. G. (1990a) Thermodynamics of the dissociation of boric acid in synthetic seawater from 273.15 to 318.15 K. *Deep Sea Res. Part A. Oceanogr. Res. Pap.* **37**, 755–766.

Dickson A. G. (1990b) Standard potential of the reaction: AgCl (s) + $12H_2$ (g) = Ag (s) + HCl (aq), and the standard acidity constant of the ion HSO_4^- in synthetic sea water from 273.15 to 318.15 K. *J. Chem. Thermodyn.* **22**, 113–127.

Dickson A. G. and Riley J. P. (1979) The estimation of acid dissociation constants in seawater media from potentionmetric titrations with strong base. I. The ionic product of water—Kw. *Mar. Chem.* **7**, 89–99.

Dickson A. G., Sabine C. L. and Christian J. R. (2007) Guide to best practices for ocean CO_2 measurements. *North Pacific Mar. Sci. Org.*, 33–39.

Dinauer A. and Mucci A. (2017) Spatial variability in surface-water pCO_2 and gas exchange in the world's largest semi-enclosed estuarine system: St. Lawrence Estuary (Canada). *Biogeosciences* **14**, 3221–3237.

Douglas N. K. and Byrne R. H. (2017) Spectrophotometric pH measurements from river to sea: Calibration of mCP for $0 \leq S \leq 40$ and $278.15 \leq T \leq 308.15$ K. *Mar. Chem.* **197**, 64–69.

Downing B. D., Boss E., Bergamaschi B. A., Fleck J. A., Lionberger M. A., Ganju N. K., Schoellhamer D. H. and Fujii R. (2009) Quantifying fluxes and characterizing compositional changes of dissolved organic matter in aquatic systems in situ using combined acoustic and optical measurements. *Limnol. Oceanogr. Methods* **7**, 119–131.

Egleston E. S., Sabine C. L. and Morel F. M. M. (2010) Revelle revisited: Buffer factors that quantify the response of ocean chemistry to changes in DIC and alkalinity. *Global Biogeochem. Cycles* **24**, 1–9.

Garcia-Mina J. M. (2006) Stability, solubility and maximum metal binding capacity in metal–humic complexes involving humic substances extracted from peat and organic compost. *Org. Geochem.* **37**, 1960–1972.

Hammer K., Schneider B., Kuliński K. and Schulz-Bull D. E. (2017) Acid-base properties of Baltic Sea dissolved organic matter. *J. Mar. Syst.* **173**, 114–121.

Hernández-Ayon J. M., Zirino A., Dickson A. G., Camiro-Vargas T. and Valenzuela-Espinoza E. (2007) Estimating the contribution of organic bases from microalgae to the titration alkalinity in coastal seawaters. *Limnol. Oceanogr. Methods* **5**, 225–232.

Holmquist J. R., Windham-Myers L., Bliss N., Crooks S., Morris J. T., Megonigal P. J., Troxler T., Weller D., Callaway J., Drexler J., Ferner M. C., Gonneea M. E., Kroeger K. D., Schile-Beers L., Woo I., Buffington K., Boyd B. M., Breithaupt J., Brown L. N., Dix N., Hice L., Horton B. P., MacDonald G. M., Moyer R. P., Reay W., Shaw T., Smith E., Smoak J. M., Sommerfield C., Thorne K., Velinsky D., Watson E., Grimes K. W. and Woodrey M. (2018) Accuracy and precision of tidal wetland soil carbon mapping in the conterminous United States. *Sci. Rep.* **8**, 9478.

Hunt C. W., Salisbury J. E. and Vandemark D. (2011) Contribution of non-carbonate anions to total alkalinity and overestimation of pCO_2 in New England and New Brunswick rivers. *Biogeosciences* **8**, 3069–3076.

Kaltin S. and Anderson L. G. (2005) Uptake of atmospheric carbon dioxide in Arctic shelf seas: evaluation of the relative importance of processes that influence pCO_2 in water transported over the Bering-Chukchi Sea shelf. *Mar. Chem.* **94**, 67–79.

Kieber R. J., Zhou X. and Mopper K. (1990) Formation of carbonyl compounds from UV-induced photodegradation of humic substances in natural waters: fate of riverine carbon in the sea. *Limnol. Oceanogr.* **35**, 1503–1515.

Kim H. and Lee K. (2009) Significant contribution of dissolved organic matter to seawater alkalinity. *Geophys. Res. Lett.* **36**, L20603.

Ko Y. H., Lee K., Eom K. H. and Han I. (2016) Organic alkalinity produced by phytoplankton and its effect on the computation of ocean carbon parameters. *Limnol. Oceanogr.* **61**, 1462–1471.

Koeve W. and Oschlies A. (2012) Potential impact of DOM accumulation on fCO_2 and carbonate ion computations in ocean acidification experiments. *Biogeosciences* **9**, 3787–3798.

Kuliński K., Schneider B., Hammer K., Machulik U. and Schulz-Bull D. (2014) The influence of dissolved organic matter on the acid–base system of the Baltic Sea. *J. Mar. Syst.* **132**, 106–115.

Lee K., Kim T. W., Byrne R. H., Millero F. J., Feely R. A. and Liu Y. M. (2010) The universal ratio of boron to chlorinity for the North Pacific and North Atlantic oceans. *Geochim. Cosmochim. Acta* **74**, 1801–1811.

Lovley D. R., Coates J. D., Blunt-Harris E. L., Phillips E. J. P. and Woodward J. C. (1996) Humic substances as electron acceptors for microbial respiration. *Nature* **382**, 445–448.

Lukawska-Matuszewska K., Grzybowski W., Szewczun A. and Tarasiewicz P. (2018) Constituents of organic alkalinity in pore water of marine sediments. *Mar. Chem.* **200**, 22–32.

Mann A. G., Kroeger K. D., O'Keefe Suttles J. A., Gonneea M. E., Brosnahan S. B. and Brooks T. W. (2019) Time-series of biogeochemical and flow data from a tidal salt-marsh creek, Sage Lot Pond, Waquoit Bay, Massachusetts (2012–2016), U.S. Geological Survey data release, https://doi.org/10.5066/P9STIROQ.

Masini J. C., Abate G., Lima E. C., Hahn L. C., Nakamura M. S., Lichtig J. and Nagatomy H. R. (1998) Comparison of methodologies for determination of carboxylic and phenolic groups in humic acids. *Anal. Chim. Acta* **364**, 223–233.

Morel F. M. M. and Hering J. G. (1993) *Principles and Applications of Aquatic Chemistry*. John Wiley & Sons Inc., New York.

Moseman-Valtierra S., Abdul-Aziz O. I., Tang J., Ishtiaq K. S., Morkeski K., Mora J., Quinn R. K., Martin R. M., Egan K., Brannon E. Q., Carey J. and Kroeger K. D. (2016) Carbon dioxide fluxes reflect plant zonation and belowground biomass in a coastal marsh. *Ecosphere* **7**, 1–21.

Muller F. L. L. and Bleie B. (2008) Estimating the organic acid contribution to coastal seawater alkalinity by potentiometric titrations in a closed cell. *Anal. Chim. Acta* **619**, 183–191.

Najjar R. G., Herrmann M., Alexander R., Boyer E. W., Burdige D. J., Butman D., Cai W. J., Canuel E. A., Chen R. F., Friedrichs M. A. M., Feagin R. A., Griffith P. C., Hinson A. L., Holmquist J. R., Hu X., Kemp W. M., Kroeger K. D., Mannino A., McCallister S. L., McGillis W. R., Mulholland M. R., Pilskaln C. H., Salisbury J., Signorini S. R., St-Laurent P., Tian H., Tzortziou M., Vlahos P., Wang Z. A. and Zimmerman R. C. (2018) Carbon budget of tidal wetlands, estuaries, and shelf waters of eastern North America. *Global Biogeochem. Cycles* **32**, 389–416.

Orr J. C., Epitalon J. M., Dickson A. G. and Gattuso J. P. (2018) Routine uncertainty propagation for the marine carbon dioxide system. *Mar. Chem.* **207**, 84–107.

Ouyang X. and Lee S. Y. (2014) Updated estimates of carbon accumulation rates in coastal marsh sediments. *Biogeosciences* **11**, 5057–5071.

Paquay F. S., Macenzie F. T. and Borges A. V. (2007) Carbon dioxide dynamics in rivers and coastal waters of the "big island" of Hawaii, USA, during baseline and heavy rain conditions. *Aquat. Geochem.* **13**, 1–18.

Paxeus N. and Wedborg M. (1985) Acid-base properties of aquatic fulvic acid. *Anal. Chim. Acta* **169**, 87–98.

Raymond P. A., Bauer J. E. and Cole J. J. (2000) Atmospheric CO_2 evasion, dissolved inorganic carbon production, and net heterotrophy in the York River estuary. *Limnol. Oceanogr.* **45**, 1707–1717.

Ritchie J. D. and Perdue E. M. (2003) Proton-binding study of standard and reference fulvic acids, humic acids, and natural organic matter. *Geochim. Cosmochim. Acta* **67**, 85–96.

Shi Z., Wang P., Peng L., Lin Z. and Dang Z. (2016) Kinetics of heavy metal dissociation from natural organic matter: Roles of the carboxylic and phenolic sites. *Environ. Sci. Technol.* **50**, 10476–10484.

Tishchenko P. Y., Wallmann K., Vasilevskaya N. A., Volkova T. I., Zvalinskii V. I., Khodorenko N. D. and Shkirnikova E. M. (2006) The contribution of organic matter to the alkaline reserve of natural waters. *Oceanology* **46**, 192–199.

Ulfsbo A., Kuliński K., Anderson L. G. and Turner D. R. (2015) Modelling organic alkalinity in the Baltic Sea using a Humic-Pitzer approach. *Mar. Chem.* **168**, 18–26.

Uyguner C. S. and Bekbolet M. (2005) Evaluation of humic acid photocatalytic degradation by UV–vis and fluorescence spectroscopy. *Catal. Today* **101**, 267–274.

van Heuven S., Pierrot D., Rae J. W. B., Lewis E. and Wallace D. W. R. (2011) MATLAB Program Developed for CO2 System Calculations. ORNL/CDIAC-105b.

Wang Z. A. and Cai W. J. (2004) Carbon dioxide degassing and inorganic carbon export from a marsh-dominated estuary (the Duplin River): A marsh CO_2 pump. *Limnol. Oceanogr.* **49**, 341–354.

Wang Z. A., Wanninkhof R., Cai W. J., Byrne R. H., Hu X., Peng T. H. and Huang W. J. (2013) The marine inorganic carbon system along the Gulf of Mexico and Atlantic coasts of the United States: Insights from a transregional coastal carbon study. *Limnol. Oceanogr.* **58**, 325–342.

Wang Z. A., Kroeger K. D., Ganju N. K., Gonneea M. E. and Chu S. N. (2016) Intertidal salt marshes as an important source of inorganic carbon to the coastal ocean. *Limnol. Oceanogr.* **61**, 1916–1931.

Yang B., Byrne R. H. and Lindemuth M. (2015) Contributions of organic alkalinity to total alkalinity in coastal waters: a spectrophotometric approach. *Mar. Chem.* **176**, 199–207.

Associate editor: Alfonso Mucci